

Comparison of Robust Control Techniques for Use in Flight Simulator Motion Bases

Mauricio Becerra-Vargas

GASI, UNESP-Univ Estadual Paulista, Campus Sorocaba, CEP 8087-180, Sorocaba, SP, Brazil

Keywords: Inverse Dynamics Control, H-Infinity Theory, Sliding Mode Control, Flight Simulator Motion Base, Stewart Platform, Parallel Robot.

Abstract: The purpose of this study is to analyse and compare three control strategies based on the inverse dynamics control structure for a six degree of freedom flight simulator motion base driven by electromechanical actuators. All strategies are applied in the outer loop of the inverse dynamic control structure by considering imperfect compensation of the nonlinearities. Imperfect compensation is intentionally introduced in order to simplify the implementation of the inverse dynamic control structure. The first strategy is just a proportional and derivative control, the second is based on Lyapunov stability theory and the third is based on H-Infinity theory. Acceleration step response and smoothness of the actuators driven torques were used to compare the performance of the controllers. The results are based on numerical simulations.

1 INTRODUCTION

Inverse dynamics control (Sciavicco and Siciliano, 2005; Spong and Vidyasagar, 2006) is an approach to nonlinear control design whose central idea is to construct an inner loop control based on the motion base dynamic model which, in the ideal case, exactly linearizes the nonlinear system and an outer loop control to drive tracking errors to zero. This technique is based on the assumption of exact cancellation of nonlinear terms. Therefore, parametric uncertainty, unmodeled dynamics and external disturbances may deteriorate the controller performance. In addition, a high computational burden is paid by computing on-line the complete dynamic model of the motion-base (Koekebakker, 2001). Robustness can be regained by applying robust control techniques in the outer loop control structure as is shown in (Becerra-Vargas and Belo, 2010; Becerra-Vargas and Belo, 2011; Becerra-Vargas and Belo, 2012).

In this context, this work presents the comparison of three control strategies applied in the outer loop of the feedback linearized system for robust acceleration tracking in the presence of parametric uncertainty and unmodeled dynamic, which is intentionally introduced in the process of approximating the dynamic model in order to simplify the implementation of this approach.

The first strategy is just a proportional and deriva-

tive control applied in the outer loop while the others two strategies introduce an additional term to the inverse dynamics controller which provides robustness to the control system. In the first strategy, the control term is designed just by providing stability, in the second, through Lyapunov stability theory and the third strategy through H-Infinity theory.

About organization of the text, this paper is structured as follows: in Section 2, the full dynamic model of motion base is presented and the inverse dynamics structure and imperfect compensation is discussed. in Section 3 and 4, the imperfect compensation is stabilize through the Lyapunov and H-Infinity theory, respectively, in Section 5 the dynamic model matrices that will be use in the controllers are defined, in Section 6 the results obtained from simulation are shown and discussed and conclusions of the present work are discussed.

2 INVERSE DYNAMIC CONTROL

In this study, a six-degree-of-freedom mechanism called the Stewart platform (Stewart, 1965) is considered. The UPS (Universal-Prismatic-Spherical) Stewart platform is composed of a moving platform linked to a fixed base through six extensible legs. Each leg is composed of a prismatic joint (i.e, an electromechanical actuator), one passive universal joint and

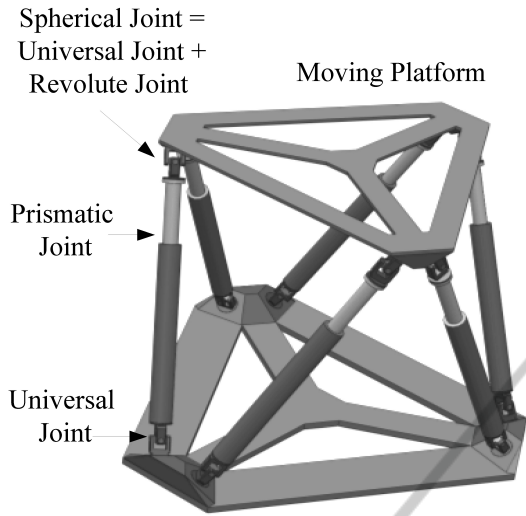


Figure 1: The UPS Stewart Platform.

one passive spherical joint making connection with the base and the moving platform (Fig. 1), respectively. Usually in flight simulators, due to mechanical design considerations, such as limited nominal load, complex design and high friction, spherical joints can be replaced (kinematically equivalent) by a universal joint and a revolute joint whose axes intersect and are non-coplanar as shown in Fig. 1.

The full dynamic model, including the kinematic and dynamic of the electromechanical actuator, in Cartesian coordinates can be given as (Becerra-Vargas and Belo, 2015):

$$\mathbf{M}(\mathbf{q})\ddot{\mathbf{q}} + \mathbf{N}(\mathbf{q}, \dot{\mathbf{q}}) = \mathbf{T}_m, \quad (1)$$

where

$$\mathbf{N}(\mathbf{q}, \dot{\mathbf{q}}) = \mathbf{C}(\mathbf{q}, \dot{\mathbf{q}}) + \mathbf{B}(\dot{\mathbf{q}}) + \mathbf{G}(\mathbf{q}), \quad (2)$$

and the Cartesian coordinates

$$\mathbf{q} = [x \ y \ z \ \phi \ \theta \ \psi]^T, \quad (3)$$

and the driving torque generated by the electromechanical actuator

$$\mathbf{T}_m = [\tau_{m_1} \ \tau_{m_2} \ \tau_{m_3} \ \tau_{m_4} \ \tau_{m_5} \ \tau_{m_6}]^T \quad (4)$$

Inverse dynamics control (Sciavicco and Siciliano, 2005; Spong and Vidyasagar, 2006) is a control law involving two feedback loops: the inner loop, which, in the ideal case, exactly linearizes the nonlinear system and the outer loop that drives tracking errors to zero. Practical implementation of the inverse dynamics control requires the parameters of the matrices $\mathbf{M}(\mathbf{q})$ and $\mathbf{N}(\mathbf{q}, \dot{\mathbf{q}})$ to be accurately known, the matrices to be modelled accurately and to be computed in real-time. These requirements are difficult to satisfy in practice. Model imprecision may come

from parametric uncertainties and purposeful choice of a simplified representation of the matrices $\mathbf{M}(\mathbf{q})$ and $\mathbf{N}(\mathbf{q}, \dot{\mathbf{q}})$ (unmodeled dynamics intentionally introduced). Therefore, the control law in the imperfect compensation case can be written as (Becerra-Vargas and Belo, 2011):

$$\mathbf{u}_T = \widehat{\mathbf{M}}(\mathbf{q})\mathbf{v} + \widehat{\mathbf{N}}(\mathbf{q}, \dot{\mathbf{q}}); \quad (5)$$

where $\mathbf{u}_T = \mathbf{T}_m$ represents the vector of voltage (which is proportional to vector torques, not considering the actuator electrical dynamics) driving the servo-drive of the electromechanical actuator, and $\widehat{\mathbf{M}}$, $\widehat{\mathbf{N}}$ represent simplified versions of \mathbf{M} , \mathbf{N} and where

$$\mathbf{v} = \ddot{\mathbf{q}}_d + \mathbf{K}_d\dot{\mathbf{e}} + \mathbf{K}_p\mathbf{e}, \quad (6)$$

and where

$$\begin{aligned} \mathbf{K}_p &= \text{diag} \{ \omega_{n1}^2, \dots, \omega_{n6}^2 \}; \\ \mathbf{K}_d &= \text{diag} \{ 2\zeta_1\omega_{n1}, \dots, 2\zeta_6\omega_{n6} \} \end{aligned} \quad (7)$$

and \mathbf{q}_d is the desired Cartesian coordinates and where the tracking error is defined as

$$\mathbf{e} = \mathbf{q}_d - \mathbf{q}, \quad (8)$$

and ω_{ni} and ζ_i characterize the response of the tracking error of the inverse dynamics control.

In order to overcome imperfect compensation effects, in this case, the simplification of the matrices \mathbf{M} and \mathbf{N} , a robust term, \mathbf{u} , is included in Eq (6), thus Eq (6) can be written as:

$$\mathbf{v} = \ddot{\mathbf{q}}_d + \mathbf{K}_d\dot{\mathbf{e}} + \mathbf{K}_p\mathbf{e} + \mathbf{u}, \quad (9)$$

Now, substituting Eq. (5) into Eq. (1) and simplifying it, one gets (Becerra-Vargas and Belo, 2011):

$$\dot{\mathbf{x}} = \mathbf{A}\mathbf{x} + \mathbf{B}(\mathbf{w} - \mathbf{u}), \quad (10)$$

where the state vector \mathbf{x} consisting of the error and its derivative is written as:

$$\mathbf{x} = [\mathbf{e} \ \dot{\mathbf{e}}]^T, \quad (11)$$

and where

$$\begin{aligned} \mathbf{w} &= (\mathbf{I} - \mathbf{M}^{-1}\widehat{\mathbf{M}})\mathbf{v} - \mathbf{M}^{-1}\Delta\mathbf{N} \\ \Delta\mathbf{N} &= \mathbf{N} - \widehat{\mathbf{N}} \end{aligned} \quad (12)$$

and

$$\mathbf{A} = (\mathbf{H} - \mathbf{BK}), \quad \mathbf{K} = [\mathbf{K}_p \ \mathbf{K}_d] \quad (13)$$

and

$$\mathbf{H} = \begin{bmatrix} \mathbf{0} & \mathbf{I} \\ \mathbf{0} & \mathbf{0} \end{bmatrix} \quad \mathbf{B} = \begin{bmatrix} \mathbf{0} \\ \mathbf{I} \end{bmatrix} \quad (14)$$

3 ROBUST CONTROL TERM, \mathbf{u} , DESIGNED BY LYAPUNOV'S SECOND METHOD

Robust control term, \mathbf{u} , was designed to stabilize the system represented by the Eq. (10) in the presence of the uncertainty \mathbf{w} , and is given as (Becerra-Vargas and Belo, 2011)

$$\mathbf{u} = \begin{cases} \frac{\rho}{\|\mathbf{z}\|} \mathbf{z} & \forall \|\mathbf{z}\| \geq \varepsilon \\ \frac{\rho}{\varepsilon} \mathbf{z} & \forall \|\mathbf{z}\| < \varepsilon \end{cases} \quad (15)$$

where

$$\mathbf{z} = \mathbf{B}^T \mathbf{P} \mathbf{x}; \quad (16)$$

and \mathbf{P} is the unique positive definite symmetric solution of

$$\mathbf{A}^T \mathbf{P} + \mathbf{P} \mathbf{A} = -\mathbf{T}, \quad (17)$$

and

$$\rho \geq \frac{1}{1-\lambda} (\lambda Q_M + \lambda \|\mathbf{K}\| \|\mathbf{x}\| + B_M \Phi) \quad (18)$$

$$\sup_{t \geq 0} \|\ddot{\mathbf{q}}_d\| < Q_M < \infty \quad \forall \ddot{\mathbf{q}}_d$$

$$\|\mathbf{I} - \mathbf{M}^{-1} \hat{\mathbf{M}}\| \leq \lambda \leq 1 \quad \forall \mathbf{q} \quad (19)$$

$$\|\Delta \mathbf{N}\| \leq \Phi < \infty \quad \forall \mathbf{q}, \dot{\mathbf{q}}$$

$$\|\mathbf{M}^{-1}\| \leq B_M \quad \forall \mathbf{q}$$

Although the control law in Eq. (15) does not guarantee error convergence to zero, it ensures bounded-norm error given by ε .

4 ROBUST CONTROL TERM, \mathbf{u} , DESIGNED BY H-INFINITY THEORY

The H-Infinity suboptimal control problem is to find a stabilizing controller $\mathbf{K}(s)$ which, based on the information in \mathbf{y} , generates a control signal \mathbf{u} which counteracts the influence of $\tilde{\mathbf{w}}$ on $\tilde{\mathbf{z}}$, thereby minimizing the closed-loop norm from $\tilde{\mathbf{w}}$ to $\tilde{\mathbf{z}}$ to less than gamma via the selected weighting function matrices, that is (Becerra-Vargas and Belo, 2012)

$$\left\| \left[\begin{array}{c} \mathbf{W}_u (\mathbf{I} + \mathbf{K} \mathbf{G})^{-1} \mathbf{K} \mathbf{G} \mathbf{W}_d \\ \mathbf{W}_e (\mathbf{I} + \mathbf{K} \mathbf{G})^{-1} \mathbf{G} \mathbf{W}_d \end{array} \right] \right\|_{\infty} < \gamma \quad (20)$$

where $\mathbf{G}(s)$ is the transfer function of the state space system defined by Eq. (10), $\mathbf{W}_e(s)$, $\mathbf{W}_d(s)$ and $\mathbf{W}_u(s)$ represent the weighting functions diagonal matrices

associated with the tracking error, disturbance (uncertainty \mathbf{w} in Eq. (12) is considered as disturbance) and control signal, respectively, and are given as

$$\mathbf{W}_e = \begin{bmatrix} W_e(s) & \dots & 0 \\ \vdots & \ddots & \vdots \\ 0 & \dots & W_e(s) \end{bmatrix}; \mathbf{W}_d = \begin{bmatrix} W_d(s) & \dots & 0 \\ \vdots & \ddots & \vdots \\ 0 & \dots & W_d(s) \end{bmatrix} \quad (21)$$

$$\mathbf{W}_u = \begin{bmatrix} W_u(s) & \dots & 0 \\ \vdots & \ddots & \vdots \\ 0 & \dots & W_u(s) \end{bmatrix}$$

It is observed from Eq. (20) that the transfer functions, $(\mathbf{I} + \mathbf{K} \mathbf{G})^{-1} \mathbf{G}$ and $\mathbf{I} + \mathbf{K} \mathbf{G}$, are two-sided weighted functions, therefore the terms A_s , A_d , A_u and M_s , M_d and M_u lower and upper bounds the spectrum of them.

5 CHARACTERISTICS OF THE DYNAMIC EQUATIONS

In flight simulators motion bases, this is due mainly to the physical restriction in terms of position, velocity and acceleration of the actuators, e.g, for low frequencies motion, the velocity and position constraints limit the maximal attainable acceleration. Moreover, the high pass wash-out filter characteristics keeps the motion system not very far away from the neutral position, to prevent the actuators from running out of stroke. Thus, the matrices $\hat{\mathbf{M}}(\mathbf{q})$ and $\hat{\mathbf{N}}(\mathbf{q})$ of the control law in Eq. (5) can be approximated to constant ones without introducing large modelling errors. Based on these constant matrices, calculation of the inverse dynamics becomes much simpler reducing computation time significantly.

In this context, matrices $\hat{\mathbf{M}}(\mathbf{q})$ and $\hat{\mathbf{N}}(\mathbf{q})$ considered in the control law in Eq. (5), are defined at the neutral position as (Becerra-Vargas and Belo, 2011; Becerra-Vargas and Belo, 2012). :

$$\begin{aligned} \hat{\mathbf{M}}(\mathbf{q}_n) &= \mathbf{K}_a^{-1} \mathbf{J}_{l,\omega}^{-T}(\mathbf{q}_n) \mathbf{M}_p(\mathbf{q}_n) \\ \hat{\mathbf{N}}(\mathbf{q}_n) &= \hat{\mathbf{G}}(\mathbf{q}_n) = \mathbf{K}_a^{-1} \mathbf{J}_{l,\omega}^{-T}(\mathbf{q}_n) \mathbf{G}_p(\mathbf{q}_n) \end{aligned} \quad (22)$$

where \mathbf{q}_n represents a neutral position and was chosen to be at half stroke of all the actuators, $\mathbf{M}_p(\mathbf{q}_n)$, $\mathbf{G}_p(\mathbf{q}_n)$, $\mathbf{J}_{l,\omega}^{-T}(\mathbf{q}_n)$ is the inertia matrix, the gravity vector and the Jacobian, respectively, calculated at the neutral position. Coriolis and centrifugal forces, and leg effects, are not considered.

6 NUMERICAL RESULTS

The performance of the controllers is verified by numerical simulations, and results are presented only for

surge (x) and the amplitude of the excitation signals (step acceleration inputs) was chosen to keep the motion base approximately 90% of the system limits in position. Desired position and acceleration are shown in Fig. 2 and Fig. 3, respectively.

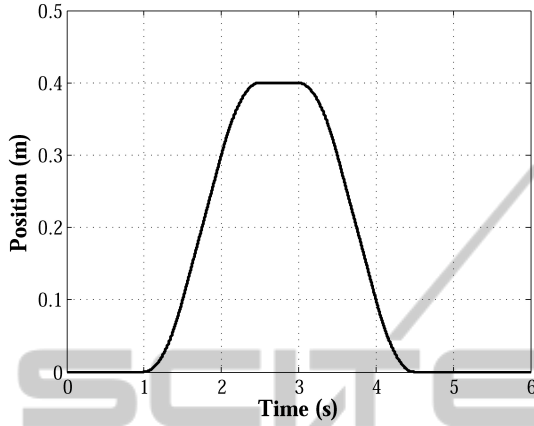


Figure 2: Desired Position - Surge (x).

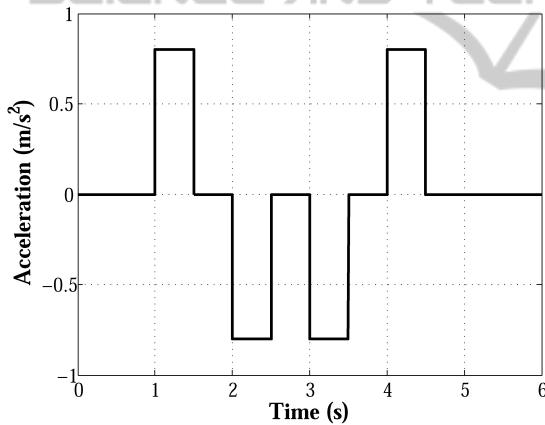


Figure 3: Desired Acceleration - Surge (x).

The sliding surface parameter ε in Eq. (15) was chosen as 0.001 (too small values can lead to instability problems). The bounding values in Eq. (19) were calculated by considering exact cancellation in the inverse control problem. Thus, $Q_M = 0.8$, $B_M = 0.27$, $\lambda = 0.72$ and $\Phi = 23$.

On the other hand, in order to yield a low-order H-Infinity controller, the penalized output signals only corresponds to the position error and the weighting functions are given as

$$W_e(s) = \frac{s/M_e + \omega_b}{s + \omega_b A_e}; \tag{23}$$

$$W_u(s) = \frac{1}{A_u}; \quad W_d(s) = A_d$$

where $M_e = 0.001$, $A_e = 1 \times 10^{-4}$, $\omega_b = 100$ Hz, $A_u = 10$ and $A_d = 6$.

With relation to the controller gains in Eq. (7), (Koekebakker, 2001) state the frequency, ω_i , should not exceed human sensory thresholds and that it should ideally be sufficiently smooth and only requires limited bandwidth (well below 1 Hz).

A bandwidth, $\omega_i = 14$ Hz and $\zeta_i = 0.6$ was chosen to the PD controller (i.e., it is considered the Eq. 6), $\omega_i = 2$ Hz and $\zeta_i = 5$ was chosen to the H-Infinity controller and $\omega_i = 6$ Hz and $\zeta_i = 1$ was chosen to the sliding mode controller (Eq. (15)).

The step acceleration response and the position error in surge direction is shown in Fig. 4 and Fig. 5, respectively. The driving torque of one actuator is shown in Fig. 6 .

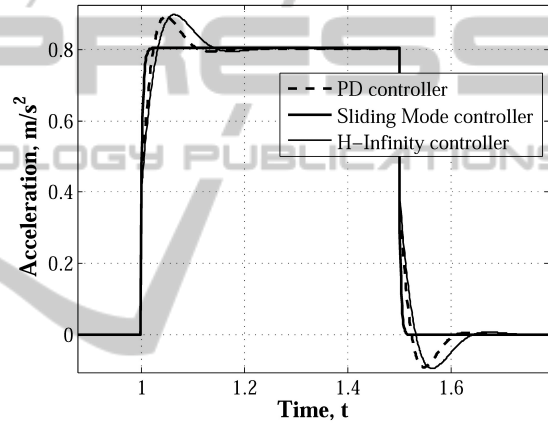


Figure 4: Acceleration response - Surge (x).

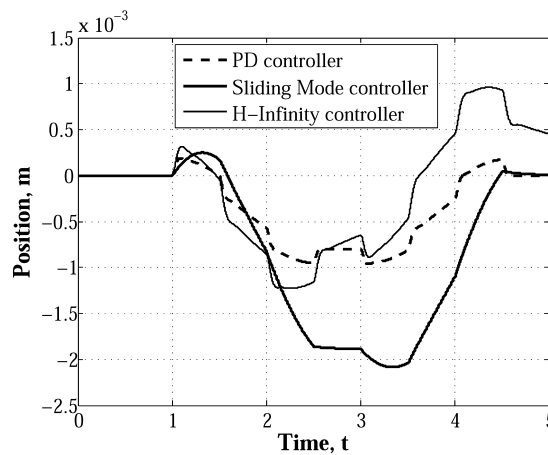


Figure 5: Position Error - Surge (x).

From these figures one can conclude the follow:

- * The sliding mode controller presented a bigger error position. As was pointed out above, this technique not guarantee error convergence to zero, but

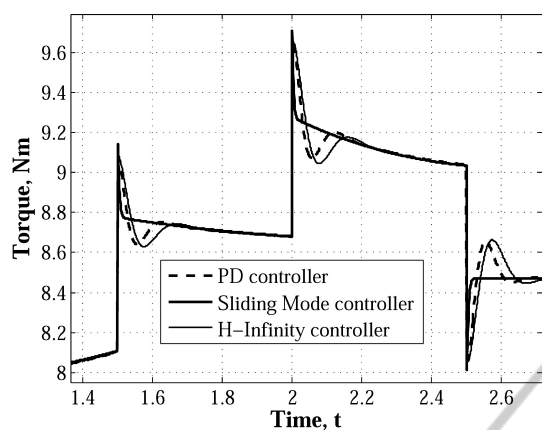


Figure 6: Driving Torque - one actuator.

it ensures bounded-norm error given by ϵ .

- * The sliding mode controller presented a rough motor torque. In this case, the principal contribution to control signal is the \mathbf{u} term, therefore by changing ω_n and ζ won't affect the response. By changing \mathbf{P} term can be produced a smoother response. Short time peak torques produce large jerk and it can lead to false cues.
- * The inverse dynamic controller without the robust term got a good response because of high gains in the controller. High gains can induce instability and noise amplification. In the other hand, high gains can produce a rough correction in the acceleration and therefore can produce false cues.
- * The H-Infinity controller presented the smoothest response but this structure leads an high order controller.

7 CONCLUSIONS

This article has presented three kinds of control approaches for the motion control of a flight simulator motion base. All controllers were implemented in the outer-loop of the inverse dynamic control scheme in order to counteract imperfect compensation. PD controller presented a rough response while the other controllers, i.e. H-infinity and sliding mode controller presented a smoother response. The reason for that behaviour is the inclusion of the robust term in the outer loop of the inverse dynamic control scheme. There is a tradeoff between the robust term and the proportional and derivative gains, causing a smoothing or rough response. Future work should be address practical implementation of these controller .

ACKNOWLEDGEMENTS

The author gratefully acknowledge the financial support provided by grant 2013/20888-6, São Paulo Research Foundation (FAPESP).

REFERENCES

- Becerra-Vargas, M. and Belo, E. (2010). Fuzzy sliding mode control of a flight simulator motion base. In *27TH Congress of the international Council of the aeronautical sciences-ICAS 2010*, pages 1–12, Nice, France. Optimage Ltd.
- Becerra-Vargas, M. and Belo, E. (2011). Robust control of a flight simulator motion base. *Journal of Guidance, Control, and Dynamics*, 34(5):1519–1528.
- Becerra-Vargas, M. and Belo, E. (2012). Application of H-Infinity theory to a 6 dof flight simulator motion base. *Journal of the Brazilian Society of Mechanical Sciences and Engineering*, 34(2):193–204.
- Becerra-Vargas, M. and Belo, E. (2015). Dynamic modeling of a 6 dof flight simulator motion base. *Journal of Computational and Nonlinear Dynamics* (doi 10.1115/1.4030013).
- Koekebakker, S. (2001). *Model based control of a flight simulator motion system*. PhD thesis, Delft University of Technology, Netherlands.
- Sciavicco, L. and Siciliano, B. (2005). *Modeling and Control of Robot Manipulators*. Springer-Verlag, Londres, 2 edition.
- Spong, M. and Vidyasagar, M. (2006). *Robot Modeling and Control*. John Wiley & Sons, New York, 1 edition.
- Stewart, D. (1965). A platform with 6 degrees of freedom. *Proceedings of the institution of mechanical engineers 1965-66*, 180(15):371–386.